Preparation of nano poly(phenylsilsesquioxane) spheres and the influence of nano-PPSQ on the thermal stability of poly(methyl methacrylate)

Xinlong Wang · Lianghu Wu · Jin Li

Abstract The nano poly(phenylsilsesquioxane) spheres (nano-PPSQ) were prepared by the sol–gel method and incorporated into poly(methyl methacrylate) (PMMA) by in situ bulk polymerization of methyl methacrylate. The structure of nano-PPSQ was confirmed by transmission electron microscope and thermogravimetry analysis (TG). The interaction between nano-PPSQ and PMMA was investigated by Fourier transform infrared spectra (FT-IR). The influence of nano-PPSQ on the thermal stability of PMMA was investigated by TG and differential scanning calorimetry (DSC) measurements. The results indicated that nano-PPSQ enhanced the thermal stability and the temperatures of glass transition (T_g) of nanocomposites. The effect of the heating rate in dynamic measurements (5–30 °C min^{-1}) on kinetic parameters such as activation energy by TG both in nitrogen and air was investigated. The Kissinger method was used to determine the apparent activation energy for the degradation of pure PMMA and nanocomposites. The kinetic results showed that the apparent activation energy for degradation of nanocomposites was higher than that of pure PMMA under air.

Keywords Nano poly(phenylsilsesquioxane) spheres · Thermal stability · Poly(methyl methacrylate) · Kinetics

Introduction

Poly(methyl methacrylate) (PMMA) is an important thermoplastic material and widely used in numerous industries such as buildings, molding, and decorative panels. However, its lower thermal stability restrains it from applications in higher temperature region. PMMA degrades to lower molecular weight compounds or to the monomer by heating or irradiating with high energy radiation. Therefore, the thermal stability of PMMA must be urgently improved to increase its commercial value. To improve the thermal properties of PMMA, fillers such as silica, titania, zirconia, and alumina, as well as clay were introduced into the PMMA [1–6].

Polysilsesquioxanes possess two unique structural features: (1) the chemical composition is a hybrid that is intermediate ($RSiO_{1.5}$) between that of silica (SiO_2) and silicones (R_2SiO); (2) polysilsesquioxanes molecules are nanoscopic in size. These materials are thermally and chemically more robust than silicones, and their nano structured shape and size provide unique properties by controlling polymer chain motion at the molecular level [7]. Polysilsesquioxanes of spherical shape can be easily prepared by the polymerization of alkyltrialkoxysilane [8]. Poly(phenylsilsesquioxane) is the most investigated polymer of the silsesquioxane class because of its good thermal stability. The presence of organic groups renders the surface of the spheres more hydrophobic than that of inorganic spheres, thus offering the potential to improve compatibility between the filler and the host polymer. Potential applications of this polymer include lithographic materials, gas-separation membranes, coatings for electronic and optical devices, especially where high temperatures are required [9].

In this article, nano poly(phenylsilsesquioxane) spheres (nano-PPSQ) were prepared, and the characterization of nano-PPSQ was performed by transmission electron microscopy (TEM) and thermogravimetry analysis (TG and DTG). PMMA/nano-PPSQ nanocomposites were prepared

X. Wang (✉) · L. Wu · J. Li
School of Chemical Engineering, Nanjing University of Science & Technology, Nanjing 210094, China
e-mail: wxinlong@sohu.com

by bulk radical polymerization of MMA in the presence of nano-PPSQ. The influence of nano-PPSQ on the thermal stability of the PMMA matrix was investigated using TG and differential scanning calorimetry (DSC). The thermal degradation kinetics of PMMA/nano-PPSQ nanocomposites was also studied.

Experimental

Materials

Phenyltrimethoxysilane (PTES, Aldrich) was used as received. Emulsifier TX-10 (alkylphenol polyoxyethylene (10) ether, MW = 646, chemical purity), acetic acid, and methanol of analytical reagent quality were purchased from Chemical Reagent Limited Corporation of National Medicine Group, China. Methyl methacrylate (MMA), *N,N*-dimethylaniline, and benzoyl peroxide (BPO) were from Shanghai Lingfeng Chemical Reagent Ltd., China. MMA was redistilled before use.

Preparation of nano-PPSQ

In a 250 mL round bottom flask fitted with a stirrer, 100 g aqueous solution of NaOH (pH = 12.5) and 1 g TX-10 were added. The mixture was heated to 50 °C, and 5 g of PTMS was carefully added dropwise with a stirring speed of 300 rpm for 30 min to ensure uniformity of the mixture. After stirring continuously for another 2.5 h at 50 °C, the mixture was cooled to room temperature, and 3 g aqueous solution of acetic acid (10 wt%) was added. The product was collected by filtration and washed three times with 100 mL deionized water and one time with 50 mL methanol. The resulting product was dried in a vacuum oven for 4 h at 60 °C.

Preparation of PMMA/nano-PPSQ nanocomposites

The 4 g of PMMA was added to 94 g of MMA, and then oscillated it for 24 h until PMMA was completely dissolved to obtain the MMA dispersion. To a 250 mL beaker, appropriate amount of nano-PPSQ, 0.1 g *N,N*-dimethylaniline, and 100 g MMA dispersion were added and stirred for 10 min. Then, 0.3 g BPO was added and stirred for 5 min. The bubbles in the contents of the beaker were removed under vacuum. Then, the mixture in the beaker was poured into the $10 \times 10 \times 0.5 \text{ cm}^3$ glass mold, and the mold was heated to 40 °C. After 24 h of polymerization at 40 °C, the plates for testing were obtained. The pure PMMA was prepared under the same experimental conditions. Using MMA dispersion instead of pure MMA for the preparation of nanocomposites could increase the viscosity of the dispersion and reduce the possibility of particle aggregation and phase separation.

Characterization

The morphologies of nano-PPSQ spheres were characterized by a JEOL-2100 TEM (Electronic Corporation, Japan). The morphologies of the PMMA/nano-PPSQ composites were observed by a Philips XL-305 FEG-SEM instrument. FT-IR spectra were recorded on a FTIR-8400S (Shimadzu Corporation, Japan) using KBr disks. DSC measurement was investigated in a nitrogen atmosphere using a Q80 DSC Apparatus (TA Corporation, America). The thermal stability of PMMA/nano-PPSQ composites was measured by non-isothermal TG method using a DTG-60/60H Simultaneous DTA–TG Apparatus (Shimadzu Corporation, Japan) from room temperature to 600 °C, and the measurements were operated at heating rates of 5, 10, 20, and 30 °C min^{-1} in nitrogen atmosphere or air in a flow rate of 20 mL min^{-1}.

Results and discussion

Preparation and characterization of nano-PPSQ spheres

The preparation of silica spheres has received considerable attention because of the development of the Stöber method, which gives rise to submicron monodisperse spherical silica spheres [10, 11]. The control of size and morphology of the spheres can be effectively controlled by changing the reaction conditions such as surfactant, the ratio of organoalkoxysilanes to water, and agitation. The morphology of the prepared spheres was shown by TEM in Fig. 1. The spheres with the diameter of about 100 nm were prepared with yield of about 90%.
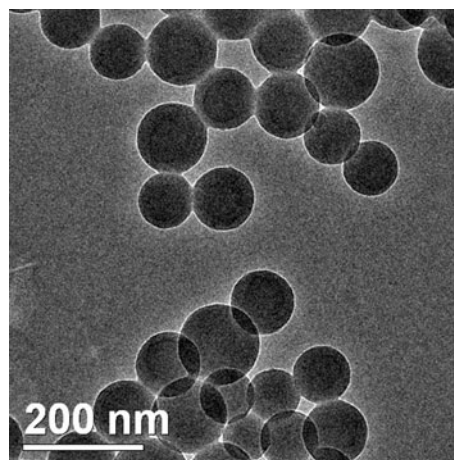

Fig. 1 The morphology of the prepared nano-PPSQ spheres

The thermal analysis would provide insight into the decomposition pathways of the particles, and such information could aid in the design of the future hybrid materials with enhanced thermal stability. As shown in Fig. 2, the particles were stable until 450 °C, and then thermal degradation occurred. The temperature for a 10% mass loss of the product was 527 °C. The presence of two distinctive mass-loss regions at 450–550 °C and 550–750 °C was clearly observed, suggesting complicated degradation processes. The mass loss of about 12% between 450 and 550 °C is probably due to the rupture of the C–H bonds and from the partial loss of organic moieties as, for example, benzene. The loss stage between 550 and 750 °C indicated further decomposition of the organic groups in particles [9].

The morphology of PMMA/nano-PPSQ nanocomposites

The compositions of PMMA/nano-PPSQ nanocomposites are listed in Table 1. The fracture surfaces of the samples were shown in Fig. 3. From the images, we can see that there was no phase separation between components, and the nano-PPSQ was well dispersed in the PMMA matrix [12].
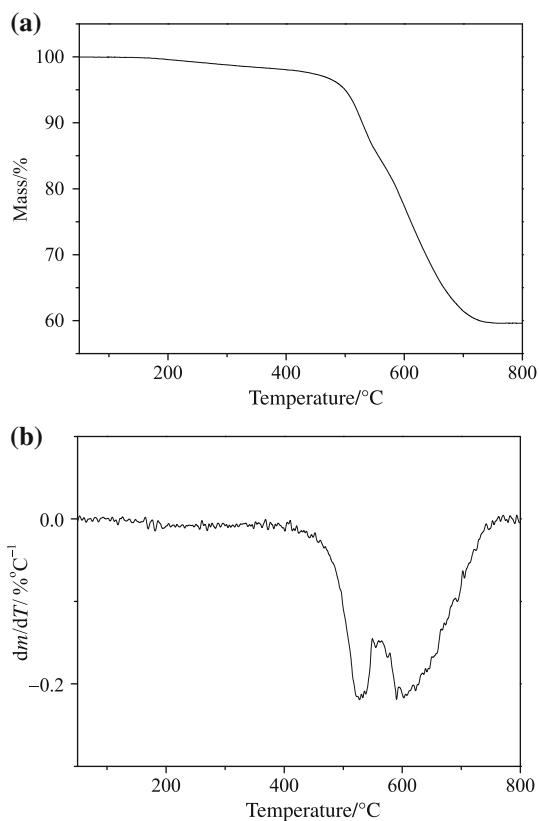
Fig. 2 The TG (**a**) and DTG (**b**) of the nano-PPSQ spheres

Table 1 The prepared PMMA/nano-PPSQ nanocomposites and the TG parameters of samples under nitrogen and air

Samples	Nano-PPSQ/ wt%	T_d/°C, nitrogen			T_d/°C, air		
		Step 1	Step 2	Step 3	Step 1	Step 2	Step 3
P0	0	205.2	285.2	354.7	177.8	253.9	360.4
P1	3.0	210.6	275.1	365.2	189.2	275.2	376.0
P2	5.0	210.3	272.3	364.4	194.8	292.4	384.2

FT-IR spectra of PMMA/nano-PPSQ nanocomposites

The properties of all heterogeneous polymer systems are determined by the same four factors: component properties, composition, structure, and interfacial interactions. Both the polymers used as matrices in particulate-filled composites and the fillers or reinforcements have the most diverse physical and chemical structures, thus a wide variety of interactions may form between them. The most important primary forces are ionic, covalent, and metallic bonds. The interactions created by van der Waals forces, i.e., by dipole–dipole (Keesom), induced dipole (Deby), and dispersion (London) interactions. They are much weaker, and the strength is between 20 and 40 kJ mol^{-1} [13]. Pure PMMA and samples of PMMA/nano-PPSQ nanocomposites were prepared by in situ bulk polymerization of MMA under the same experimental conditions. The infrared spectra of pure PMMA and nanocomposites were shown in Fig. 4. The pure PMMA shows the carbonyl absorption at 1729.4 cm^{-1}, while of the composites with nano-PPSQ, the carbonyl absorption begins to shift to a lower wave number, for 5% nano-PPSQ at 1720.0 cm^{-1}[14]. A significant difference in the wave number of the carbonyl absorption means that there was interaction between the nano-PPSQ and the PMMA matrix [15].

The T_g of the nanocomposites

The glass transition behavior of the nanocomposites was investigated by DSC. The DSC curves of the samples were shown in Fig. 5. From Fig. 5, it can be seen that the values increased with the addition of the nano-PPSQ. When filled with 3% nano-PPSQ, the T_g of PMMA is improved from 112.7 to 121.7 °C. It is well known that there are many factors affecting the T_g of polymer, such as the flexible of the main chain, the type of substituents, and the configuration. The introduction of the nano-PPSQ restricted the mobility of the polymer chains and accordingly, a significant shift in the T_g of PMMA towards higher temperature was observed [6]. This agrees well with the results of FT-IR spectra analysis.

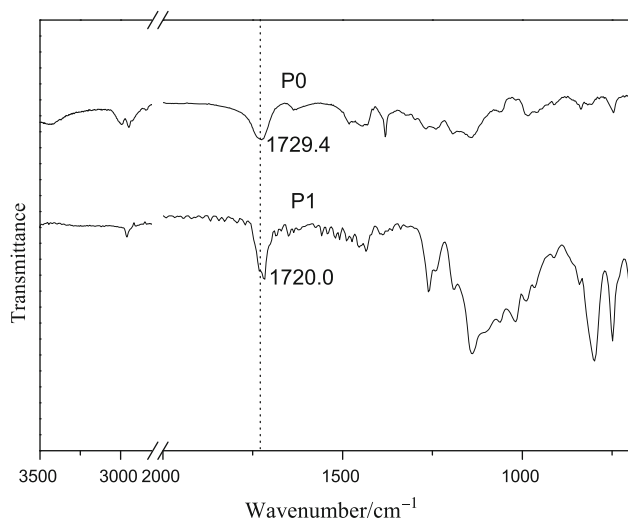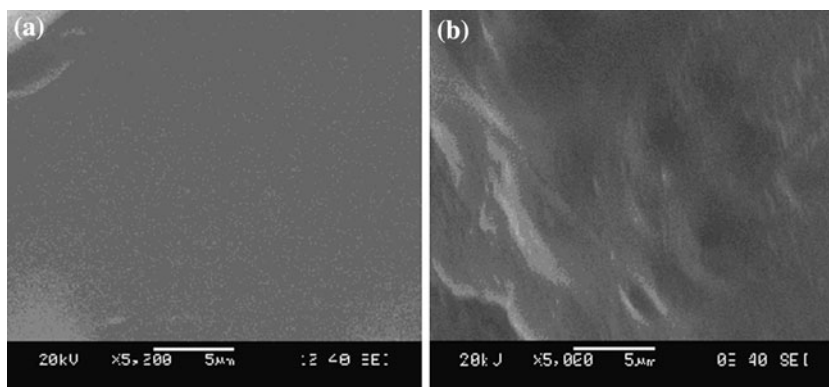Fig. 3 The morphology of PMMA/nano-PPSQ composites (**a**:P0; **b**:P1)

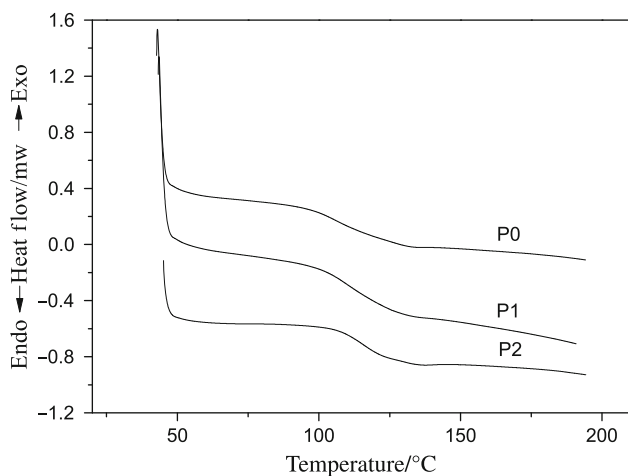Fig. 4 The FT-IR spectra of pure PMMA and PMMA/nano-PPSQ

Fig. 5 The DSC curves of the nanocomposites

Fig. 6 The TG (**a**) and DTG (**b**) curves of nano-PPSQ composites in nitrogen

Thermal stability and thermal degradation kinetics of PMMA/nano-PPSQ nanocomposites

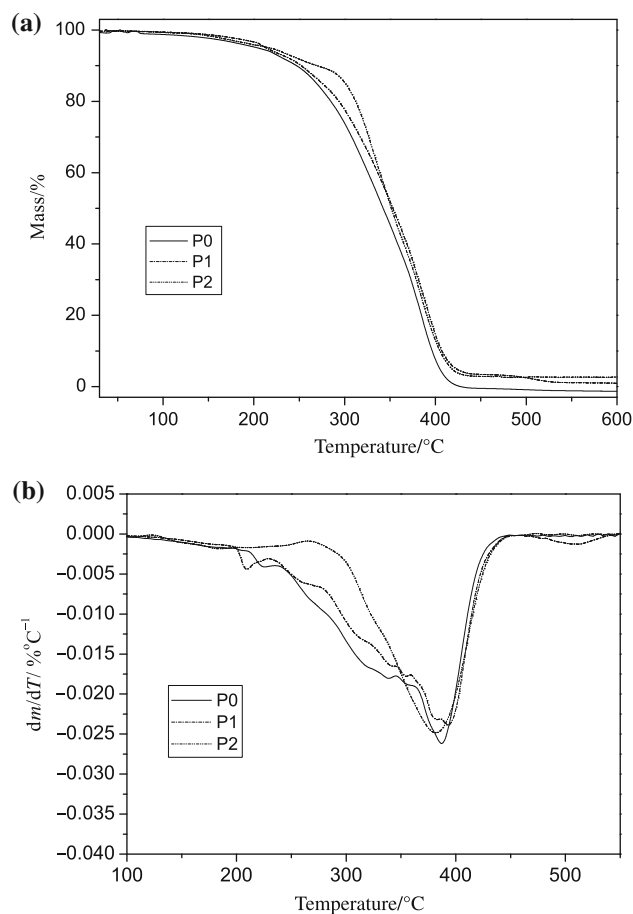The effect of nanoparticles on increasing the thermal stability of polymeric materials was proposed through several mechanisms such as the barrier effect in which nanoparticles retard heat and mass transport necessary for the degradation process. Furthermore, the thermal stability was also reported to be enhanced by the restriction of the polymer chain mobility in particle/polymer composites [16]. Yoshida reported that the thermal degradation temperature of PMMA/nano-SiO_2 composites increased with increasing nano-SiO_2 fraction, and then decreased after the maximum, in the range at around 2–8 wt% of nano-SiO_2.
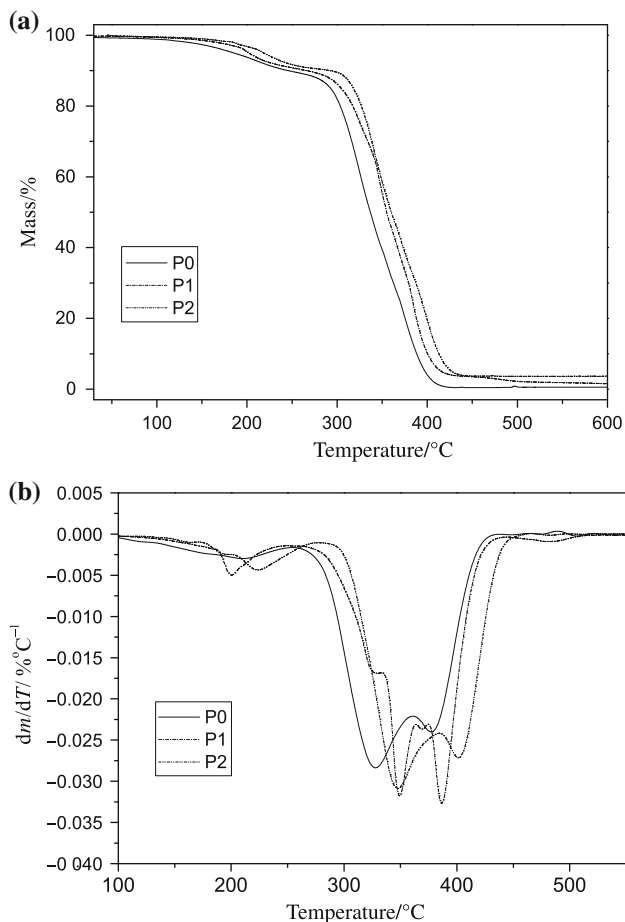
(a)

(b)

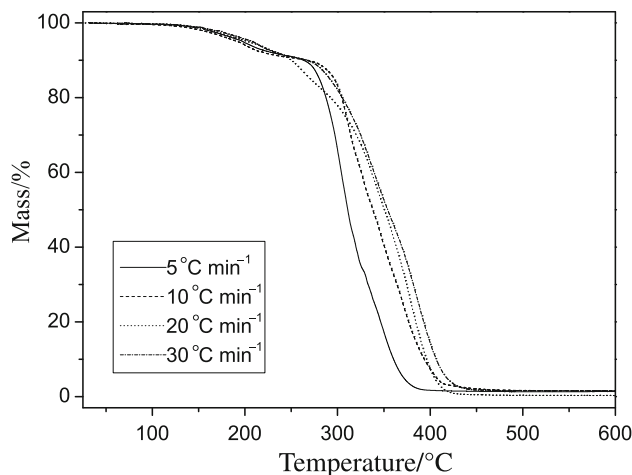Fig. 7 The TG (**a**) and DTG (**b**) curves of nano-PPSQ composites in air

Fig. 8 TG curves of pure PMMA at different heating rates under nitrogen

Fig. 9 TG curves of pure PMMA at different heating rates under air

Fig. 10 TG curves of nanocomposites (P1) at different heating rates under nitrogen

The nano particle size also influenced the thermal stability improvement of PMMA, the thermal stability increased with decreasing the particle size [17]. The thermal stability of PMMA/nano-PPSQ nanocomposites was tested by TG. The TG and DTG curves of the samples under nitrogen and air were shown in Figs. 6 and 7, respectively. From the Figs. 6 and 7, it can be seen that the thermal degradation of pure PMMA and nearly all the PMMA/nano-PPSQ nanocomposites showed three stages correspondence with the cleavage of head-to-head linkages, unsaturated vinyl ends, and the random scission of PMMA main chains [18, 19]. The initial decomposition temperatures (T_d) of each step were listed in Table 1. Under nitrogen, the T_ds of the three steps for pure PMMA are about 205.2, 285.2, and 354.7 °C, but when nano-PPSQ is introduced, the T_d for the first step and the T_d for the third step increases. However, the T_d for the second step decreases. Under air, the T_ds of the three steps for pure PMMA are about 177.8, 253.9, and 360.4 °C, but when nano-PPSQ is introduced, the T_ds for all three steps increase obviously. Besides, the increasing range in air is larger than that under nitrogen. With 3.0 wt% of nano-PPSQ (P1), the increase in T_d was about

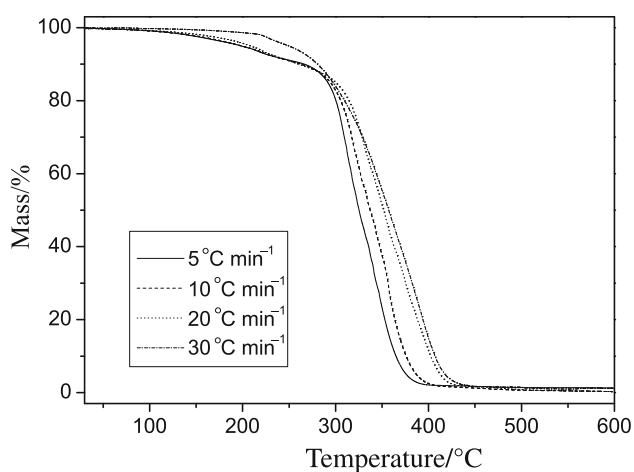**Fig. 11** TG curves of nanocomposites (P1) at different heating rates under air

5.4, 9.9, and 10.5 °C for the three stages in nitrogen, but the values were 11.4, 21.5, and 15.6 °C, respectively, under air atmosphere. The improvement in thermal stability is caused by chain restriction, and this may be proved by the results of glass transition temperature as shown in Fig. 5. Glass transition temperature (T_g) is directly related to the polymer chain mobility. If nanoparticles are added to the polymer, then they will obstruct polymer chain motion and T_g will increase [16].

TG curves of the pure PMMA and PMMA/nano-PPSQ composites performed under nitrogen and air at heating

rates of 5, 10, 20, and 30 °C min^{-1} were shown in Figs. 8, 9, 10, and 11 respectively. In order to evaluate the degradation kinetics, the Kissinger method was employed to analyze the TG data. Kissinger has put forward, during the degradation of polymers, a simple but accurate relationship among apparent activation energy (E_a), temperature of the maximum reaction rate at a constant heating rate (T_p) obtained from the DTG curves and listed in Table 2, and heating rate (β) as follows [20]:

$$\frac{d \ln(\frac{\beta}{T_p^2})}{d(\frac{1}{T_p})} = -\frac{E_a}{R}. \tag{1}$$

Plots of $-\ln(\beta/T_p^2)$ against $(1/T_p)$ could be created using the integral form of the Eq. 1, and the activation energy (E_a) can be calculated from the slope of the line. The $-\ln(b/T_p^2)$ as $1/T_p$ plots were obtained with good linearity and accuracy. The activation energies (E_a) of every stage for pure PMMA and nanocomposites are listed in Table 2. Under nitrogen, the E_as of the first stage and the third stage for nanocomposites are larger than that of pure PMMA, but the E_a for the stage two is slightly lower than that of pure PMMA. Under air, when the nano-PPSQ is blended into PMMA, the three decomposition processes of nanocomposites all show larger values of E_a compared with pure PMMA. The increase in the apparent activation energy can be explained by the action of nano-PPSQ which could inhibit the depolymerization of PMMA. Also under air, the

Table 2 The activation energies (E_a) of every stage for pure PMMA and nanocomposites

Samples	Heating rate/°C min^{-1}	T_p/°C			Activation energy, E_a/KJ mol^{-1}	Correlation coefficient (γ)
		Stage 1	Stage 2	Stage 3		
P0						
Air	5	–	308	355	103.09 (Stage 1)	1
	10	202	310	365	76.56 (Stage 2)	0.9505
	20	214	326	377	120.42 (Stage 3)	0.9951
	30	213	339	394		
Nitrogen	5	–	306	348	115.02 (Stage 1)	1
	10	197	312	371	133.94 (Stage 2)	0.9858
	20	218	343	377	138.28 (Stage 3)	0.9958
	30	214	340	388		
P1						
Air	5	–	309	349	118.49 (Stage 1)	1
	10	217	320	373	106.62 (Stage 2)	0.9932
	20	231	340	380	136.91 (Stage 3)	0.9897
	30	229	339	395		
Nitrogen	5	–	309	360	119.05 (Stage 1)	1
	10	220	328	371	128.18 (Stage 2)	0.9891
	20	229	345	389	182.24 (Stage 3)	0.9960
	30	229	350	396		

E_a of the second stage for PMMA is lower than that of the first stage, and this indicates that oxygen may enhance the degradation of PMMA at high temperature but suppresses the degradation at lower temperature. From Table 2, it can also be seen that the E_as of the three stages for PMMA and nanocomposites in air are lower than those under nitrogen because of the oxygen's participation [21].

Conclusions

The PMMA/nano-PPSQ nanocomposites samples with different amounts of nano-PPSQ were synthesized by bulk radical polymerization of methyl methacrylate. TG results both in nitrogen and air showed that the thermal decomposition temperature (T_d) of each step was affected with loading of nano-PPSQ. The TG kinetics results by the Kissinger method showed that the apparent activation energies of the degradation of pure PMMA were lower than that of nanocomposites in air, indicating that nano-PPSQ had an effect on the degradation process of PMMA. The introduction of the nano-PPSQ restricted the mobility of the polymer chains and enhanced the T_g of nanocomposites.

References

1. Marinovic-Cincovic M, Popovic MC, Novakovic MM, Nedeljkovic JM. The influence of β-FeOOH nanorods on the thermal stability of poly (methyl methacrylate). Polym Degrad Stab. 2007;92:70–4.
2. Laachachia A, Cocheza M, Ferriola M, Lopez-Cuestab JM, Leroy E. Influence of TiO_2 and Fe_2O_3 fillers on the thermal properties of poly(methyl methacrylate) (PMMA). Mater Lett. 2005;59:36–9.
3. Kuan HC, Chiu SL, Chen CH, Kuanl CF, Chiang CL. Synthesis, characterization, and thermal stability of PMMA/SiO_2/TiO_2 tertiary nanocomposites via non-hydrolytic sol–gel method. J Appl Polym Sci. 2009;113:1959–65.
4. Kandare E, Deng HM, Wang DY, Hossenlopp JM. Thermal stability and degradation kinetics of poly(methyl methacrylate)/layered copper hydroxymethacrylate composites. Polym Adv Technol. 2006;17:312–9.
5. Chatterjee A. Effect of nanoTiO_2 addition on poly(methyl methacrylate): an exciting nanocomposites. J Appl Polym Sci. 2010;116:3396–407.
6. Lerari D, Peeterbroeck S, Benali S, Benaboura A, Dubois P. Use of a new natural clay to produce poly(methylmethacrylate)-based nanocomposites. Polym Int. 2010;59:71–7.
7. Sankaraiah S, Lee JM, Kim JH. Preparation and characterization of surface-functionalized polysilsesquioxane hard spheres in aqueous medium. Macromolecules. 2008;41:6195–204.
8. Kim YB, Kim YA, Yoon KS. Preparation of functionalized polysilsesquioxane and polysilsesquioxane-metal nanoparticle composite spheres. Macromol Rapid Commun. 2006;27:1247–53.
9. Takahashi K, Tadanaga K, Matsuda A, Hayashi A, Tatsumisago M. Thermoplastic and thermosetting properties of polyphenylsilsesquioxane spheres prepared by two-step acid-base catalyzed sol-gel process. J Sol-Gel Sci Technol. 2007;41:217–22.
10. Arkhireeva A, Hay JN. Synthesis of sub-200 nm silsesquioxane particles using a modified Stöber sol–gel route. J Mater Chem. 2003;13:3122–7.
11. Arkhireev A, Hay JN, Oware W. A versatile route to silsesquioxane nanospheres organically modified silane precursors. J Sol-Gel Sci Technol. 2005;51:1688–95.
12. Takeshi O, Yoshiki C. Poly(methyl methacrylate) (PMMA)-based hybrid materials with reactive zirconium oxide nanocrystals. Polym J. 2010;42:58–65.
13. Janos M, Bela P. Polymer micro and nanocomposites: structure, interactions, properties. J Ind Eng Chem. 2008;14:535–63.
14. Dimitris SA, Alexandros KN, George PK. PMMA/organomodified montmorillonite nanocomposites prepared by in situ bulk polymerization. J Therm Anal Calorim. 2010;102:451–60.
15. Feng Y, Jia Y, Xu HY. Preparation and thermal properties of hybrid nanocomposites of poly(methyl methacrylate)/octavinyl polyhedral oligomeric silsesquioxane blends. J Appl Polym Sci. 2009;111:2684–90.
16. Wantinee V, Richard LL. Effect of nanoparticles on the thermal stability of PMMA nanocomposites prepared by in situ bulk polymerization. J Therm Anal Calorim. 2011;103:267–73.
17. Zou DQ, Yoshida H. Size effect of silica nanoparticles on thermal decomposition of PMMA. J Therm Anal Calorim. 2010;99:21–6.
18. Manring LE, Sogah DY, Cohen GM. Thermal degradation of poly(methyl methacrylate). 3. Polymer with head-to-head linkages. Macromolecules. 1989;22(12):4652–4.
19. Hirata T, Kashiwagi T, Brown JE. Thermal and oxidative degradation of poly(methyl methacrylate): weight loss. Macromolecules. 1985;18(7):1410–8.
20. Kissinger HE. Reaction kinetics in differential thermal analysis. Anal Chem. 1957;29(11):1702–6.
21. Arisawa H, Brill TB. Kinetics and mechanisms of flash pyrolysis of poly(methyl methacrylate) (PMMA). Combust Flame. 1997;109(3):415–26.